Microporous and Mesoporous Materials 207 (2015) 90–94

Contents lists available at ScienceDirect

Microporous and Mesoporous Materials

journal homepage: www.elsevier.com/locate/micromeso

# $H_2S$ interaction with HKUST-1 and ZIF-8 MOFs: A multitechnique study

Jayashree Ethiraj [a], Francesca Bonino [a, *], Carlo Lamberti [b, c], Silvia Bordiga [a]

[a] Department of Chemistry, NIS and INSTM Reference Centre, University of Turin, Via G. Quarello 15, I-10135 and Via P. Giuria 7, I-10125 Turin, Italy
[b] Southern Federal University, Zorge Street 5, 344090 Rostov-on-Don, Russia
[c] Department of Chemistry, CrisDi Centre for Crystallography, University of Torino, Via Giuria 7, I-10125 Torino, Italy

ARTICLE INFO

*Article history:*
Received 24 October 2014
Received in revised form
22 December 2014
Accepted 28 December 2014
Available online 13 January 2015

*Keywords:*
Metal-organic frameworks
Hydrogen sulfide
IR spectroscopy
Raman spectroscopy
X-ray diffraction

ABSTRACT

The interaction of $H_2S$ with HKUST-1 and ZIF-8 MOFs has been studied by means of FT-IR, Raman, DRUV-Vis-NIR and PXRD techniques. At very low equilibrium pressure (below 5 mbar) a stepwise structural distortion is observed in both HKUST-1 and ZIF-8. At higher equilibrium pressures (20–60 mbar), PXRD technique, in particular, showed the structural destruction of HKUST-1 with formation of a covallite (CuS) phase and some structural distortion of ZIF-8.



## 1. Introduction

Hydrogen sulphide ($H_2S$) is a colourless, toxic and flammable gas, that needs to be removed from gas mixtures used in the energy sector as it acts as poison in respect of most of the precious metal catalysts [1]. At the present time both physical and chemical absorption media use aqueous solvents like amine solutions (monoethanolamine (MEA), diethanolamine (DEA) and methyldiethanolamine (MDEA)), potassium carbonate solution, alkaline activated carbons, zeolites [2–4]. Metal-organic frameworks (MOFs), known for their high porosity and structural flexibility, [5–6] have shown reversible adsorption towards $H_2S$ gas. Some of the well studied MOFs are MIL-53(Al, Cr, Fe), MIL-47(V), MIL-100(Cr), and MIL-101(Cr) [7–9] and CPO-27-Ni [10]. MOFs comprising a tridimensional succession of motifs, with metal ions in 2+/3+/4 + states, have been found to be stable in the presence of water or humidity and they exhibit a high sulphur selectivity and strong chemical resistance to the corrosive sulphur gases; and can be regenerated without high energetic regeneration costs [11].

HKUST-1, first reported in 1999 is a well studied material [12] where $Cu^{2+}$ ions form dimers, each copper atom is coordinated by four oxygens of the benzene-1,3,5-tricarboxilate (BTC) linkers and by one water molecule. Single-crystal data have shown that it forms face centred cubic crystals that contains a large square-shaped pores (9.9 Å). The presence of water molecule in the first coordination sphere of copper ions can be removed by dehydration creating coordinative vacancy on $Cu^{2+}$ species. The coordinative unsaturation of metal centres after thermal treatments and interaction with probe molecules like NO, $CO_2$, CO, $N_2$ and $H_2$ have reported in Refs. [13–15]. Moreover, HKUST-1 has been well studied for other gases like ammonia [16]. The interaction of small molecules with the coordinatively unsatured metal centres of the HKUST-1 by means of density functional theory have been studied for CO, $CO_2$, OCS, $SO_2$, NO, $NO_2$, $N_2O$, $NH_3$, $PH_3$ and other small molecules [17]. Some experimental evidence of $H_2S$ interaction with HKUST-1 is reported by Petit et al., where they have proposed a mechanism of degradation of HKUST-1 upon $H_2S$ adsorption [18–20]. On the other hand, Gutierrez–Sevillano et al. [21] have studied $H_2S$ adsorption on three well known MOFs, namely HKUST-1, MIL-47(V), and IRMOF-1(Zn). According to their study, the $H_2S$ adsorption energy in the case of HKUST-1, is −43.4 (kJ $mol^{-1}$) which is lower than $H_2O$ adsorption energy of −46.7 (kJ $mol^{-1}$) and they claim that there must be something missing in the mechanisms proposed so far to explain the degradation observed in the MOF upon adsorption of $H_2S$. Theoretical studies on CPO-27-Ni have also shown higher interaction energy for $H_2O$ than $H_2S$ [10].

* Corresponding author.
*E-mail address:* francesca.bonino@unito.it (F. Bonino).

http://dx.doi.org/10.1016/j.micromeso.2014.12.034
1387-1811/

The second MOF of this study, ZIF-8 (Zeolitic Imidazolate Framework) [22,23] is porous and crystalline framework in which the tetrahedral metal ions are linked by imidazolate (Im) units. ZIF structures may be compared with those of zeolites, as the bridging angle formed by this linkage is analogous to that between silicon oxygen and aluminium oxygen units in zeolites. ZIF-8 as a promising storage material was investigated at high pressures up to ~39 GPa by in situ FTIR spectroscopy [24]. Apart from characterization, nanosized ZIF-8 has been studied and proved to be a reusable esterification catalyst [25] and the latest study on functionalization of ZIF-8 by using malonitrile has been reported for $H_2S$ fluorescent detection and highly selective amino acid recognition [26].

In the present contribution we report a multitechnique study (FT-IR, Raman, DRUV-Vis-NIR, PXRD) on the $H_2S$ interaction with HKUST-1 and ZIF-8. Based on our experience, the multitechnical approach is very useful in the characterization of complex materials such as MOFs [27–29].

## 2. Experimental

MOF samples, HKUST-1(Basolite™ C300) and ZIF-8 (Basolite™ Z1200) were purchased by Sigma–Aldrich. The samples were activated in vacuo at 423 K and 573 K respectively.

FT-IR spectra were collected on a Nicolet-6700 spectrometer equipped with a MCT B type detector, in the range of 4000–400 $cm^{-1}$, in transmission mode with a 2 $cm^{-1}$ resolution. The samples have been prepared as self-supported thin pellets.

UV-Vis-NIR spectra have been collected in Diffuse Reflectance mode on a Cary5000 Varian spectrophotometer equipped with a reflectance sphere. All the samples have been measured in powder form in a suprasil quartz homemade optical bulb cell which allows measurement in controlled atmosphere.

Raman spectra were recorded on a Renishaw inVia Raman microscope spectrometer. Unfortunately the two samples revealed a different fluorescence behaviour depending on the laser line and therefore two different laser lines were used. In particular an $Ar^+$ laser emitting at 514 nm and a diode laser emitting at 785 nm were used for HKUST-1 and ZIF-8 respectively. Photons scattered by the sample were dispersed by a 1800 (514 nm) and 1200 (785 nm) lines/mm grating monochromator and were simultaneously collected on a CCD camera; the collection optic was set at 20X objective. The spectral collection setup consisted of 50 acquisitions, each of 10 s.

X-ray Powder Diffraction (PXRD) patterns have been collected with a PW3050/60 X'Pert PRO MPD diffractometer from PANalytical working in Debye–Scherrer geometry, using a high power ceramic tube PW3373/10 LFF with a Cu anode equipped with Ni filter to attenuate $K_\beta$ and focused by X-ray mirror PW3152/63. Scattered photons have been collected by a RTMS (Real Time Multiple Strip) X'celerator detector. The samples have been measured as powders inside a 0.8 mm boronsilicate capillary in air.

## 3. Results and discussion

### 3.1. FT-IR spectroscopy

#### 3.1.1. Activation of the samples [27]

Fig. 1a shows FT-IR spectra of HKUST-1 in air and activated at 423 K for 1 h. The spectrum of the hydrated sample is clearly dominated by large amount of solvent in the 3800–2000 $cm^{-1}$ region. In the dehydrated form IR absorption bands of the BTC linker are observed in 1800–400 $cm^{-1}$ range [13]. The out of scale absorption bands in the range 1700–1500 $cm^{-1}$ and 1500–1300 $cm^{-1}$ correspond to $\nu_{asym}(C{-}O_2)$ and $\nu_{sym}(C{-}O_2)$ [13–16]. The other very intense absorption band is centred at 738 $cm^{-1}$ and it was previously assigned [13–16] to $\nu$(C–H) bending mode. In the considered range only the band centred at 505 $cm^{-1}$ is assigned to a vibrational mode directly involving the Cu centre. Following the previous interpretations, [13–16] this feature is assigned to Cu–O stretching mode.

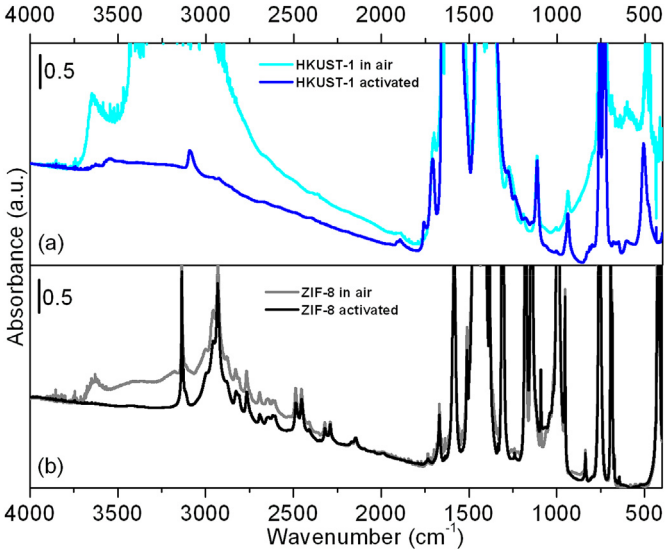


**Fig. 1.** a) FT-IR spectra of in air (cyan curve) and activated at 423 K for 1 h (blue curve) HKUST-1; b) FT-IR spectra of in air (dark grey) and activated at 573 K for 2 h (black curve) ZIF-8. (For interpretation of the references to colour in this figure legend, the reader is referred to the web version of this article.)

Fig. 1b shows ZIF-8 in air and activated at 573 K for 2 h. Solvent used in the synthesis (DMF) and water are easily removed upon thermal activation in vacuo. The broad band centred at 3000 $cm^{-1}$ due to the presence of some hydrogen bond between MOF functional groups with solvent disappears, while ZIF-8 fingerprint vibrational modes become clearly distinguishable. At higher frequency the activated ZIF-8 shows two contributions: the first one centred at 3134 $cm^{-1}$ and the second one in the 3000–2850 $cm^{-1}$ range, ascribable to C–H stretching vibrational modes respectively of the ring and of the methyl group present in the 2-methylimidazole linker. The peak at 1586 $cm^{-1}$ can be assigned as the C=N stretch mode specifically, whereas the intense and convoluted bands at 1500–1350 $cm^{-1}$ are associated with the entire ring stretching [24]. The bands in the spectral region of 1350–900 $cm^{-1}$ are for the in-plane bending of the ring while those below 800 $cm^{-1}$ are assigned as out-of-plane bending [24]. As expected, clearly, a very intense band at 421 $cm^{-1}$ due to Zn–N stretching mode is clearly observed [24].

#### 3.1.2. $H_2S$ adsoprtion on HKUST-1 and ZIF-8

FT-IR spectra of HKUST-1 contacted, after activation, with increasing dosages of $H_2S$ (up to $p_{eq}$ = 10 mbar) are reported in Fig. 2a. Surprisingly, and differently from the CPO-27-Ni case [10], the three IR active vibrational modes of molecular $H_2S$ at 2626, 2614, and 1182 $cm^{-1}$, corresponding to the asymmetric, symmetric stretching, and bending vibrational modes, are totally absent. The interaction results in a progressive growing up of very broad and indefinite bands, in the 3700–2100, 1750–1100 and 950–650 $cm^{-1}$ range. Moreover the band at 505 $cm^{-1}$ due to the Cu–O vibrational mode [13–16] is gradually eroded. All these evidences are the first signal of a probable HKUST-1 framework instability upon interaction with $H_2S$.

In the case of ZIF-8 (Fig. 2b), $H_2S$ dosage is stopped at $p_{eq}$ = 5 mbar (dark yellow curve), due to the extreme fragility of the

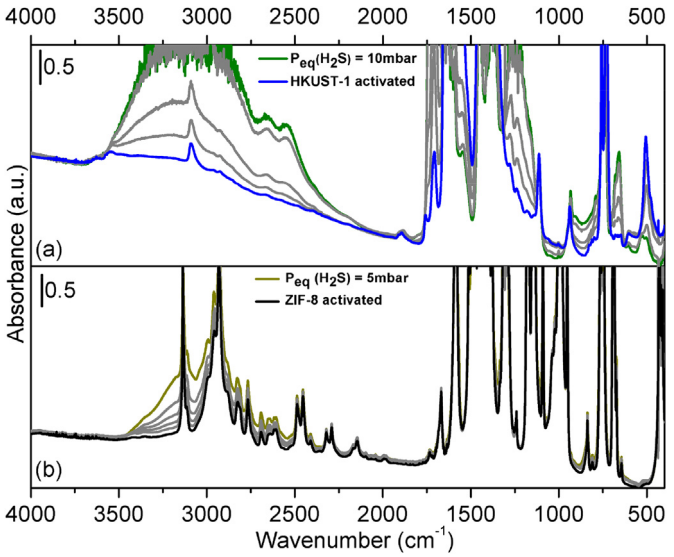


**Fig. 2.** FT-IR spectra reporting increasing adsorption dosages of $H_2S$ (from grey to olive/dark yellow curves) on activated HKUST-1 (part a) blue curve) and ZIF-8 (part b) black curve). (For interpretation of the references to colour in this figure legend, the reader is referred to the web version of this article.)

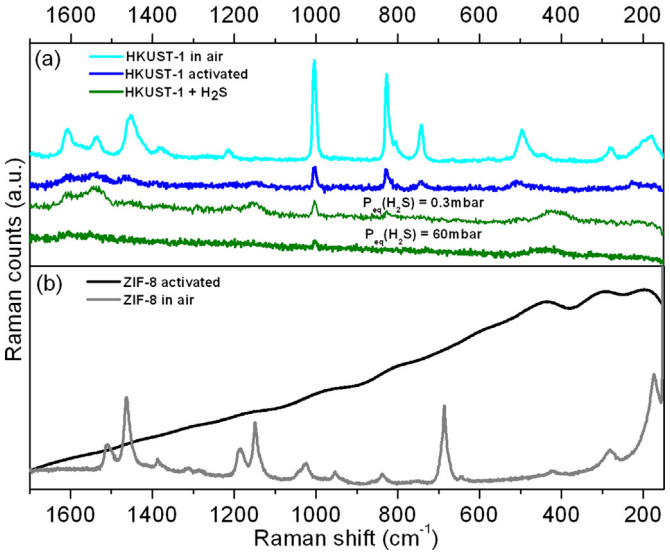


**Fig. 3.** Raman spectra of a): in air (cyan curve), activated (blue curve) and interacting with $H_2S$ (olive curves) HKUST-1 ($\lambda$ = 514 nm); b): in air (grey curve) and activated (black curve) ZIF-8 ($\lambda$ = 785 nm). (For interpretation of the references to colour in this figure legend, the reader is referred to the web version of this article.)

pellet at higher adsorbate pressures. Very differently from HKUST-1, all the vibrational modes in the low frequency range (1700–400 $cm^{-1}$) are unperturbed. However, again $H_2S$ vibrational modes are hardly recognized and in the higher frequency range (3500–2550 $cm^{-1}$), less markedly than in HKUST-1 case, broad bands appear, overlapping ZIF-8 vibrational fingerprints. This fact can be probably simply due to the presence of hydrogen bonded species and not to the MOF decomposition (at least this is the evidence at this coverage by means of IR spectroscopy).

### 3.2. Raman spectroscopy

Vibrational Raman spectra (in the 1700–150 $cm^{-1}$ range) of both HKUST-1 and ZIF-8 have also been acquired (Fig. 3). Part a) reports the Raman spectra of as such (cyan curve), activated (blue curve) and interacting with $H_2S$ (olive curves) HKUST-1. As previously reported, the as such sample spectrum is dominated by the organic linker contribution. The bands at 1610 $cm^{-1}$ and 1004 $cm^{-1}$ are associated with $\nu$(C=C) modes of the benzene ring; the peaks at 828 $cm^{-1}$ and 742 $cm^{-1}$ are ascribed to out-of-plane ring (C–H) bending vibrations and to out-of-plane ring bending, respectively. The bands at 1536 $cm^{-1}$ and 1452 $cm^{-1}$ are due to the $\nu_{asym}$(C–$O_2$) and $\nu_{sym}$(C–$O_2$) units. The bands at 496 $cm^{-1}$, 280 $cm^{-1}$ and 190 $cm^{-1}$ correspond to vibrational modes directly involving Cu(II) species. Unfortunately, activation leads to deterioration of the signal to noise ratio of the measured spectrum. However, while the dehydration process of HKUST-1 MOF does not affect the high-frequency modes of the organic part of the framework, it is evident that the modes in the 600–150 $cm^{-1}$ range, ascribed to vibrational modes involving Cu(II) species, are dramatically perturbed by water removal. In particular the band at 496 $cm^{-1}$ shifts to 508 $cm^{-1}$ and a peak at 224 $cm^{-1}$ appears. These two contributions are assigned respectively to Cu–O and Cu–Cu vibrational modes [13–16]. Progressive dosages of $H_2S$ cause almost the total disappearance of all the HKUST-1 bands and the growing of a new very broad band centred at 415 $cm^{-1}$. It is quite evident, more than in the case of IR technique, that, upon interaction with $H_2S$, HKUST-1 loses all its fingerprint vibrational modes and a new Cu–S species, responsible for the appearance of the band at lower frequency, [30] is formed.

Part b) of Fig. 3 reports Raman spectra of ZIF-8. The sample in air (grey curve) shows the typical Raman fingerprint of ZIF-8. Very strong bands were observed at 173 $cm^{-1}$, 686 $cm^{-1}$, 1149 $cm^{-1}$, and 1463 $cm^{-1}$ corresponding to Zn–N stretching, imidazole ring puckering, C5–N stretching and methyl bending, respectively [31]. Unfortunately, in this case, it is not possible to study the vibrational perturbations upon $H_2S$ dosages, as already the activated sample gives very strong fluorescence covering all the possible Raman signals in the considered range.

### 3.3. DRUV-Vis-NIR spectroscopy

As previously reported by us [13–16] HKUST-1, upon activation changes drastically its colour from light cyan to blue navy. After interaction with $H_2S$ the sample turns to dark green colour (see Fig. 4a1).

This trend can be explained only if a change in the coordination sphere of copper is invoked, as the colour is associated with d–d transitions of Cu(II) ions (see Fig. 4a2).

The spectrum of the sample in air (cyan curve) shows the already known features, that are (i) an edge around 350 nm due to a ligand to metal charge transfer (LMCT) transition from oxygen to copper atoms and (ii) a band centred at 708 nm, characteristic of the d–d transition for Cu(II) species in a distorted octahedral local geometry. Upon activation at 423 K (blue curve), a shoulder in the d–d band centred at 609 nm, a red shift of the maximum, previously observed at 708 nm, to 719 nm and of the absorption associated with the LMCT transition are observed. The change in the d–d region is ascribed to the activation of new available d–d transitions due to a loss of degeneracy in d levels produced by a change in the symmetry around copper. The LMCT edge shift is explained as a consequence of the change of (i) the hydration conditions of the carboxylated group and (ii) the coordination sphere of copper ions.

Upon a small dosage of $H_2S$ (grey curve), the octahedral geometry is perturbed and the spectrum goes back to that observed in case of sample in air with a strong decrease in the intensity of the

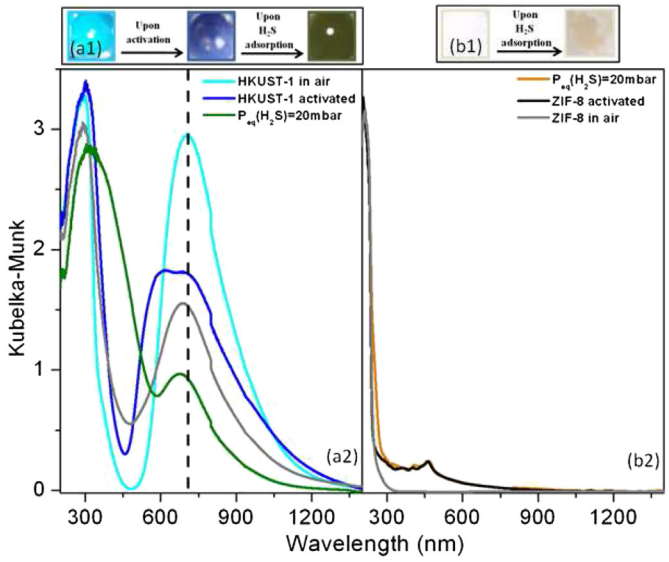


**Fig. 4.** Part a1) and b1) images corresponding to HKUST-1 and ZIF-8 in air, activated and interacting with $H_2S$. DRUV-Vis-NIR spectra of HKUST-1 (part a2)) in air (cyan curve), activated (blue curve) and interacting with $H_2S$ (grey and olive curves) and of ZIF-8 (part b2)) in air (grey curve), activated (black curve) and interacting with $H_2S$ (dark yellow curve). (For interpretation of the references to colour in this figure legend, the reader is referred to the web version of this article.)

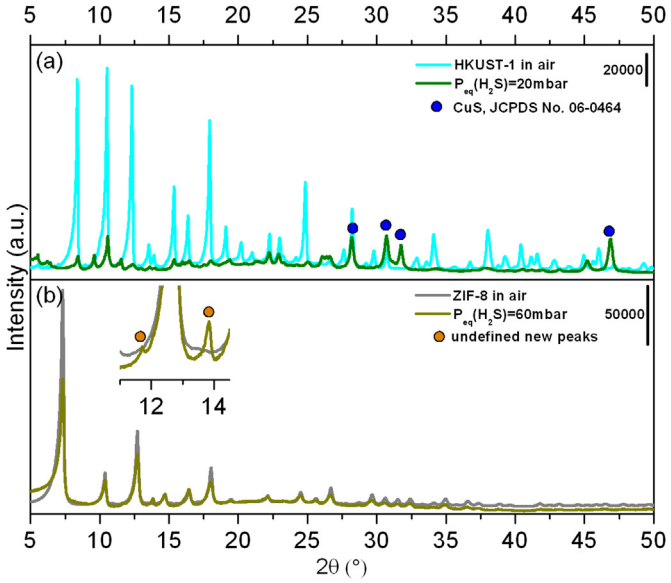


**Fig. 5.** PXRD patterns of HKUST-1 in air and after interaction with $H_2S$ (part a), cyan and olive curves) and ZIF-8 (part b), grey and dark yellow curves). Reflections labelled with full circles represent new phases. (For interpretation of the references to colour in this figure legend, the reader is referred to the web version of this article.)

band at 708 nm. When the interaction occurs with 20 mbar of $H_2S$, the LMCT shifts to 470 nm and the d-d band blue-shifts to 687, with significant decrease in intensity. These experimental evidences, again, show that the coordination sphere of copper is strongly perturbed upon $H_2S$ interaction.

Moving now to ZIF-8, the sample, upon $H_2S$ interaction, changes only slightly colour, from white to very pale yellow (see Fig. 4b1). Thus, DRUV-Vis spectra of ZIF-8 (Fig. 4b2) interacting with $H_2S$ (dark yellow curve) are less informative than in the previous case. In fact the spectrum is almost superimposed to that one of the activated sample (black curve). Also the passage from the sample in air (grey curve) to the activated form reveals small differences. In particular, upon activation, besides the very intense band with edge at 240 nm, due to electronic transitions involving the linker itself or LMCT from the linker nitrogen atoms to zinc atoms, a new small multi-component contribution appears centred at 400 nm.

### 3.4. Powder X-ray diffraction

As expected from previous results, upon $H_2S$ dosage, HKUST-1 x-ray diffraction pattern is completely destroyed and new well defined reflections (blue full circle symbols) appear (see Fig. 5a). Looking at literature data, [32] they can be easily assigned to covellite CuS. This is the final proof that $H_2S$ is reacting with copper centres, forming a new compound, that is covellite, and demolishing HKUST-1 framework.

In case of ZIF-8, the effect of $H_2S$ interaction, is very less destructive, even at pressure higher than for HKUST-1 (see Fig. 5b). A small number of new reflections (orange full circle symbols) appear at low angles (see the inset). Unfortunately their assignment is not straightforward and they do not correspond to any sulphide phase involving zinc. Due to the very low intensity of such unassigned reflections, the fraction of the sample volume concerned by this phase transformation is negligible.

## 4. Conclusions

HKUST-1 and ZIF-8 interacting with $H_2S$ have been characterized by means of FTIR, Raman, DRUV-Vis and PXRD techniques.

HKUST-1 clearly showed a strong perturbation of all the vibrational, electronic and structural fingerprints due to the formation of a covellite CuS phase and consequent destruction of the framework. On the contrary, ZIF-8 revealed to be more stable, undergoing only to a slight framework perturbation. In this case PXRD technique showed the presence of new small reflections, not ascribable to any sulphide involving zinc atom, that however concerns a negligible fraction of sample, being the dominant fraction of ZIF-8 unchanged by $H_2S$ adsorption.

## Acknowledgements

This work has been supported by EU FP-7 Framework NANOMOF project under grant agreement CP-IP 228604-2. C.L. acknowledges the Mega-grant of the Russian Federation Government to support scientific research at Southern Federal University, No. 14.Y26.31.0001.

## References

[1] R. Pellegrini, G. Agostini, E. Groppo, A. Piovano, G. Leofanti, C. Lamberti, J. Catal. 280 (2011) 150–160.
[2] R. Yan, T. Chin, Y.L. Ng, H. Duan, D.T. Liang, J.H. Tay, Environ. Sci. Technol. 38 (2004) 316–323.
[3] W. Yuan, T.J. Bandosz, Fuel 86 (2007) 2736–2746.
[4] X. Wang, X. Ma, X. Xu, L. Sun, C. Song, Top. Catal. 49 (2008) 108–117.
[5] G. Ferey, C. Serre, T. Devic, G. Maurin, H. Jobic, P.L. Llewellyn, G. De Weireld, A. Vimont, M. Daturi, J.S. Chang, Chem. Soc. Rev. 40 (2011) 550–562.
[6] H. Furukawa, K.E. Cordova, M. O'Keeffe, O.M. Yaghi, Science 341 (2013) 1230444.
[7] L. Hamon, H. Leclerc, A. Ghoufi, L. Oliviero, A. Travert, J.-C. Lavalley, T. Devic, C. Serre, G. Ferey, G. De Weireld, A. Vimont, G. Maurin, J. Phys. Chem. C 115 (2011) 2047–2056.
[8] L. Hamon, C. Serre, T. Devic, T. Loiseau, F. Millange, G. Ferey, G. De Weireld, J. Am. Chem. Soc. 131 (2009) 8775–8777.
[9] A. Peluso, N. Gargiulo, P. Aprea, F. Pepe, D. Caputo, Sci. Adv. Mater. 6 (2014) 164–170.

[10] S. Chavan, F. Bonino, L. Valenzano, B. Civalleri, C. Lamberti, N. Acerbi, J.H. Cavka, M. Leistner, S. Bordiga, J. Phys. Chem. C 117 (2013) 15615–15622.
[11] T. Devic, G. De Weireld, G. Ferey, L. Hamon, T. Loiseau, C. Serre, Patent numbers: WO2009130251-A2, 2009; WO2009130251-A3, 2010; EP2268382-A2, 2011; JP2011520592-W, 2011; US2012085235-A1, 2012.
[12] S.S.Y. Chui, S.M.F. Lo, J.P.H. Charmant, A.G. Orpen, I.D. Williams, Science 283 (1999) 1148–1150.
[13] C. Prestipino, L. Regli, J.G. Vitillo, F. Bonino, A. Damin, C. Lamberti, A. Zecchina, P.L. Solari, K.O. Kongshaug, S. Bordiga, Chem. Mater. 18 (2006) 1337–1346.
[14] S. Bordiga, L. Regli, F. Bonino, E. Groppo, C. Lamberti, B. Xiao, P.S. Wheatley, R.E. Morris, A. Zecchina, Phys. Chem. Chem. Phys. 9 (2007) 2676–2685.
[15] K.S. Lin, A.K. Adhikari, C.N. Ku, C.L. Chiang, H. Kuo, Int. J. Hydrogen Energy 37 (2012) 13865–13871.
[16] E. Borfecchia, S. Maurelli, D. Gianolio, E. Groppo, M. Chiesa, F. Bonino, C. Lamberti, J. Phys. Chem. C 116 (2012) 19839–19850.
[17] B. Supronowicz, A. Mavrandonakis, T. Heine, J. Phys. Chem. C 117 (2013) 14570–14578.
[18] C. Petit, B. Mendoza, T.J. Bandosz, ChemPhysChem 11 (2010) 3678–3684.
[19] C. Petit, T.J. Bandosz, Dalton Trans. 41 (2012) 4027–4035.
[20] C. Petit, B. Levasseur, B. Mendoza, T.J. Bandosz, Microporous Mesoporous Mater. 154 (2012) 107–112.
[21] J.J. Gutierrez-Sevillano, A. Martin-Calvo, D. Dubbeldam, S. Calero, S. Hamad, RSC Adv. 3 (2013) 14737–14749.
[22] X.C. Huang, Y.Y. Lin, J.P. Zhang, X.M. Chen, Angew. Chem. Int. Ed. 45 (2006) 1557–1559.
[23] W. Morris, C.J. Stevens, R.E. Taylor, C. Dybowski, O.M. Yaghi, M.A. Garcia-Garibay, J. Phys. Chem. C 116 (2012) 13307–13312.
[24] Y. Hu, H. Kazemian, S. Rohani, Y.N. Huang, Y. Song, Chem. Commun. 47 (2011) 12694–12696.
[25] L.H. Wee, T. Lescouet, J. Ethiraj, F. Bonino, R. Vidruk, E. Garrier, D. Packet, S. Bordiga, D. Farrusseng, M. Herskowitz, J.A. Martens, ChemCatChem 5 (2013) 3562–3566.
[26] H. Li, X. Feng, Y. Guo, D. Chen, R. Li, X. Ren, X. Jiang, Y. Dong, B. Wang, Sci. Rep. 4 (2014) 4366.
[27] F. Bonino, C. Lamberti, S. Chavan, J.G. Vitillo, S. Bordiga, in: F.X. Llabres i Xamena, J. Gascon (Eds.), Metal Organic Frameworks as Heterogeneous Catalysts, The Royal Society of Chemistry, Cambridge, 2013, pp. 76–142 ch. 4.
[28] E. Borfecchia, D. Gianolio, G. Agostini, S. Bordiga, C. Lamberti, in: F.X. Llabres i Xamena, J. Gascon (Eds.), Metal Organic Frameworks as Heterogeneous Catalysts, The Royal Society of Chemistry, Cambridge, 2013, pp. 143–208 ch. 5.
[29] S. Bordiga, F. Bonino, K.P. Lillerud, C. Lamberti, Chem. Soc. Rev. 39 (2010) 4885–4927.
[30] J. Alvarez-Garcia, E. Rudigier, N. Rega, B. Barcones, R. Scheer, A. Perez-Rodriguez, A. Romano-Rodriguez, J.R. Morante, Thin Solid Films 431 (2003) 122–125.
[31] G. Kumari, K. Jayaramulu, T.K. Maji, C. Narayana, J. Phys. Chem. A 117 (2013) 11006–11012.
[32] K. Tezuka, W.C. Sheets, R. Kurihara, Y.J. Shan, H. Imoto, T.J. Marks, K.R. Poeppelmeier, Solid State Sci. 9 (2007) 95–99.